Electronic Supplementary Material (ESI) for Journal of Materials Chemistry B.

Supporting Information

Planar-Structured Thiadiazoloquinoxaline-Based NIR-II Dye for Tumor Phototheranostics

Liangyu Zheng[1], Ziqi Zhao[1], Chun Xue[1], Lei An[1], Weidan Na[2*], Fan Gao[1], Jinjun Shao[3], Changjin Ou[1*]

[1]Institute of Advanced Materials and Flexible Electronics (IAMFE), School of Chemistry and Materials Science, Nanjing University of Information Science and Technology, Nanjing, China.

Email: ocj1987@163.com

[2]College of Chemistry and Chemical Engineering, Xuzhou University of Technology, Xuzhou, 221111, China.

Email: wdna@xzit.edu.cn

[3]Key Laboratory of Flexible Electronics (KLOFE) and Institute of Advanced Materials (IAM), Nanjing Tech University (NanjingTech), Nanjing, China.

Experimental Section

Materials

All chemicals and reagents were purchased commercially Shanghai Titan Technology Co., Ltd without further purification. All air and moisture sensitive reaction were carried out in flame-dried glassware under a nitrogen protection. ^{1}H (400 MHz) and ^{13}C (100 MHz) nuclear magnetic resonance spectra were record on a JNM-ECZ400S/L1 spectrometer using tetramethylsilane (TMS) in $CDCl_3$ as an internal standard. Mass spectra were performed on autoflex speed MALDI-TOF.

Synthetic route of compound 1: A 100 mL Schlenk flask was charged with methyl 2-bromothiophene-3-carboxylate (1.03 g, 9.32 mmol), benzo[b]thiophen-2-ylboronic acid (3.32 g, 18.65 mmol), K_2CO_3 (2.58 g, 18.64 mmol), KF (1.75 g, 18.64 mmol) and $Pd(PPh_3)_4$ (538 mg, 0.47 mmol). After degassed by three vacuum pump cycles and backfilled with nitrogen, deionized water (12 mL) and THF (20 mL) were added and the mixture was stirred at 60 °C for 12 h. After diluted with 20 mL water, the mixture was extracted with dichloromethane and the organic phase was dried by anhydrous $MgSO_4$. The solvent was removed under reduced pressure, and the crude residual was purified by silica gel column chromatography with dichloromethane and hexane mixture as eluent yielding methyl 2-(benzo[b]thiophen-2-yl)thiophene-3-carboxylate as a white solid (2.06 g, 80.6 %). ^{1}H NMR (400 MHz, $CDCl_3$) δ 7.86 -7.74 (m, 2H), 7.69 (s, 1H), 7.51 (d, *J* = 5.4 Hz, 1H), 7.40 - 7.31 (m, 2H), 7.27 (d, *J* = 5.4 Hz, 1H), 3.83 (s, 3H). ^{13}C NMR (100 MHz, $CDCl_3$) δ 163.50, 143.05, 140.86, 139.61, 134.07, 130.63, 128.56, 125.88, 125.06, 124.62, 124.15, 122.00, 51.91.

Synthetic route of compound 2: A 100 mL two-necked round-bottom flask was charged with 1-bromo-4-butylbenzene (6.40 g, 30.04 mmol) and dried THF (20 mL). After degassed by three

vacuum pump cycles and backfilled with nitrogen, the solution was cooled down to -78 °C and stirred for 10 min. The n-butyllithium (1.6 M in hexane, 18.3mL, 29.29 mmol) was added slowly by using a syringe, and the resulting mixture was stirred at -78 °C for 1 h. Thereafter, **1** (2.06 g, 7.51 mmol) was added and the mixture was stirred for another 5 min at -78 °C and stirred at room temperature overnight. After the addition of 100 mL saturated NH_4Cl aqueous solution, the mixture was extracted by dichloromethane. The organic phase was dried with anhydrous $MgSO_4$ and the solvent was evaporated under reduced pressure. The crude product was used without further purification. A 50mL Schlenk flask was charged with the crude product**,** amberlyst15 ion-exchange resin (388 mg) and dichloromethane (10 mL). The mixture was stirred at room temperature for 7 hours. Then the solvent was evaporated under reduced pressure. The crude product was purified by silica gel column chromatography with dichloromethane and hexane mixture as eluent yielding **2** as a light-yellow solid (1.83 g, 49.5 %). ^{1}H NMR (400 MHz, $CDCl_3$) δ 7.88 - 7.77 (m, 1H), 7.51 (dd, *J* = 6.3, 1.4 Hz, 1H), 7.24 - 7.17 (m, 3H), 7.13 (d, *J* = 8.3 Hz, 4H), 7.08 (d, *J* = 4.9 Hz, 1H), 7.02 (d, *J* = 8.6 Hz, 4H), 2.53 (t, *J* = 5.9 Hz, 4H), 1.57 - 1.53 (m, 2.1 Hz, 4H), 1.36 - 1.30 (m, 4H), 0.89 (t, *J* = 7.3 Hz, 6H). ^{13}C NMR (100 MHz, $CDCl_3$) δ 161.44, 150.44, 143.21, 141.53, 139.52, 137.38, 136.63, 134.84, 128.48, 128.25, 126.94, 124.80, 123.86, 123.12, 123.05, 121.83, 62.57, 35.32, 33.56, 22.57, 14.09.

Synthetic route of compound 3: A solution of **2** (1.23 g, 2.50 mmol) in 10 mL DMF was added dropwise into NBS (1.0 M in DMF, 2.62 mL, 2.62 mmol) and the resulting mixture was stirred at 0 °C for 5 h. After diluted with 50 mL water, the mixture was extracted with dichloromethane and the organic phase was dried with anhydrous $MgSO_4$. Then the solvent was evaporated under reduced pressure. The crude product was purified by silica gel column chromatography with

dichloromethane and hexane mixture as eluent yielding **3** as a dark-yellow oil (1.36 g, 95.4 %). ^{1}H NMR (400 MHz, $CDCl_3$) δ 7.94 - 7.74 (m, 1H), 7.49 (d, *J* = 8.1 Hz, 1H), 7.24 - 7.18 (m, 2H), 7.16 - 7.07 (m, 5H), 7.03 (d, *J* = 8.5 Hz, 4H), 2.53 (t, *J* = 7.8 Hz, 4H), 1.58 - 1.53 (m, 4H), 1.36 - 1.29 (m, 4H), 0.90 (t, *J* = 7.3 Hz, 6H). ^{13}C NMR (100 MHz, $CDCl_3$) δ 160.06, 149.85, 143.26, 141.81, 138.80, 136.98, 136.76, 134.52, 128.61, 128.17, 126.09, 124.95, 123.89, 123.42, 121.91, 113.15, 63.25, 35.34, 33.57, 22.59, 14.11.

Synthetic route of compound 4: A 20 mL two-necked round-bottom flask was charged with **3** (210 mg, 0.37 mmol) and dried THF (5 mL). After degassed by three vacuum pump cycles and backfilled with nitrogen, the solution was cooled down to -78 °C and stirred for 10 min. The n-butyllithium (1.6 M in hexane, 0.28 mL, 0.44 mmol) was added slowly by using a syringe, and the resulting mixture was stirred at -78 °C for 1 h. Thereafter, tributyltin chloride (0.12 mL, 0.44 mmol) was added and the mixture was stirred for another 5 min at -78 °C and stirred at room temperature overnight. After the addition of 20 mL saturated aqueous KF, the mixture was extracted with dichloromethane three times. The organic phase was combined, dried with anhydrous $MgSO_4$ and the solvent was evaporated under reduced pressure. The crude product was used without further purification.

Synthetic route of compound TP-DBBT: A 20 mL Schlenk flask was charged with **4**, 4,8-Dibromobenzo[1,2-c:4,5-c']bis([1,2,5]thiadiazole) (130 mg, 0.37 mmol) and $Pd(PPh_3)_4$ (86 mg, 0.074 mmol). After degassed by three vacuum pump cycles and backfilled with nitrogen, dried toluene (4 mL) was added and the mixture was stirred at 100 °C for overnight. After cooling down to room temperature, water was added, and the mixture was washed with dichloromethane three

times. The organic phase was combined and dried with anhydrous $MgSO_4$. After the removal of the solvent under reduced pressure, the crude product was purified by column chromatography on silica gel with dichloromethane and hexane mixture as eluent yielding **TP-DBBT** as a yellow solid (66 mg, 13.1 %). ^{1}H NMR (400 MHz, $CDCl_3$) δ 9.28 (s, 2H), 7.90 - 7.85 (m, 2H), 7.62 - 7.55 (m, 2H), 7.34 -7.27 (m, 12H), 7.10 (d, *J* = 8.5 Hz, 8H), 2.55 (t, *J* = 7.8 Hz, 8H), 1.56 - 1.51 (m, 8H), 1.36 - 1.30 (m, 8H), 0.89 (t, *J* = 7.3 Hz, 12H). ^{13}C NMR (101 MHz, $CDCl_3$) δ 162.92, 154.61, 153.02, 150.48, 145.47, 144.49, 141.91, 139.24, 137.81, 134.62, 132.46, 132.36, 131.68, 129.70, 128.68, 128.59, 128.48, 125.18, 124.16, 124.10, 122.61, 118.11, 63.17, 35.39, 33.59, 22.64, 14.10.

Synthetic route of compound 5: A 20 mL two-necked round-bottom flask was charged with **3** (230 mg, 0.40 mmol) and dry THF (4 mL). After degassed by three vacuum pump cycles and backfilled with nitrogen, the solution was cooled down to -78°C and stirred for 10 min. The n-butyllithium (1.6 M in hexane, 0.5 mL, 0.80 mmol) was added slowly by using a syringe, and the resulting mixture was stirred at -78 °C for 1 h. Thereafter, 2-isopropoxy-4,4,5,5-tetramethyl-1,3,2-dioxaborolane (223 mg, 1.20 mmol) was added and the mixture was stirred for another 5 min at -78 °C and stirred at room temperature overnight. After the addition of 20 mL saturated aqueous NH_4Cl, the mixture was extracted by dichloromethane. The organic phase was dried with anhydrous $MgSO_4$ and the solvent was evaporated under reduced pressure. The crude product was used without further purification.

Synthetic route of compound 6: A 50 mL Schlenk flask was charged with **5**, 4,7-dibromo-5,6-dinitrobenzo[c][1,2,5]thiadiazole (184 mg, 0.48 mmol), K_2CO_3 (138 mg, 1 mmol) and $Pd(PPh_3)_4$ (55 mg, 0.048 mmol). After degassed by three vacuum pump cycles and backfilled with nitrogen,

deionized water (4 mL), Toluene (2 mL) and THF (8 mL) were added and the mixture was stirred at 100 °C for 12 h. After diluted with 10 mL water, the mixture was extracted with dichloromethane and the organic phase was dried with anhydrous $MgSO_4$. After the removal of the solvent under reduced pressure, the crude product was purified by silica gel column chromatography with dichloromethane and hexane mixture as eluent yielding **6** as a blue solid (148 mg, 61.3 %). ^{1}H NMR (400 MHz, $CDCl_3$) δ 7.92 - 7.79 (m, 2H), 7.64 - 7.57 (m, 2H), 7.52 (s, 2H), 7.33 - 7.26 (m, 4H), 7.17 (d, *J* = 8.2 Hz, 8H), 7.07 (d, *J* = 8.3 Hz, 8H), 2.55 (t, *J* = 7.8 Hz, 8H), 1.59 - 1.52 (m, 8H), 1.37 - 1.31 (m, 8H), 0.90 (t, *J* = 7.3 Hz, 12H). ^{13}C NMR (100 MHz, $CDCl_3$) δ 161.72, 152.72, 151.73, 144.24, 144.16, 142.10, 141.07, 138.56, 136.47, 134.44, 131.03, 128.70, 128.22, 126.46, 125.19, 124.28, 124.05, 122.68, 120.02, 63.25, 35.34, 33.56, 22.59, 14.09.

Synthetic route of compound 7: A 50 mL two-necked round-bottom flask was charged with **6** (50 mg, 0.04 mmol), zinc powder (31 mg, 0.48 mmol) and NH_4Cl (13 mg, 0.24 mmol). After degassed by three vacuum pump cycles and backfilled with nitrogen, DCM (4 mL) and MeOH (2mL) were added, the mixture was stirred at room temperature for 5 h. The organic phase was filtered through Celite pad and the solvent was evaporated under reduced pressure. The crude product was used without further purification.

Synthetic route of compound TP-TQ1: A 20 mL Schlenk flask was charged with **8**, benzil (25 mg, 0.12 mmol). After degassed by three vacuum pump cycles and backfilled with nitrogen, acetic acid (4 mL) was added and the mixture was stirred at 100 °C for overnight. After cooling down to room temperature, water was added, and the mixture was washed with dichloromethane three times. The organic phase was combined and dried with anhydrous $MgSO_4$. After the removal of the

solvent under reduced pressure, the crude product was purified by column chromatography on silica gel with dichloromethane and hexane mixture as eluent yielding **TP-TQ1** as a dark-green solid (30 mg, 56.8 %). ^{1}H NMR (400 MHz, $CDCl_3$) δ 9.20 (s, 2H), 7.86 (d, *J* = 7.4 Hz, 2H), 7.79 (d, *J* = 7.0 Hz, 4H), 7.57 (d, *J* = 7.8 Hz, 2H), 7.50 - 7.44 (m, 2H), 7.41 (t, *J* = 7.3 Hz, 4H), 7.36 - 7.26 (m, 10H), 7.22 (d, *J* = 8.8 Hz, 2H), 7.07 (d, *J* = 8.5 Hz, 8H), 2.54 (t, *J* = 7.8 Hz, 8H), 1.57 - 1.52 (m, 8H), 1.35 - 1.31 (m, 8H), 0.88 (t, *J* = 7.3 Hz, 12H). ^{13}C NMR (100 MHz, $CDCl_3$) δ 161.37, 151.56, 150.78, 144.46, 143.26, 142.49, 141.40, 139.86, 139.75, 138.52, 135.49, 134.87, 132.47, 130.61, 129.22, 128.45, 128.37, 126.48, 124.90, 124.03, 123.54, 122.86, 122.26, 120.24, 62.99, 35.37, 33.54, 22.70, 14.13.

Synthetic route of compound TP-TQ2: A 20 mL Schlenk flask was charged with **8** and Phenanthrene-9,10-dione (25 mg, 0.12 mmol). After degassed by three vacuum pump cycles and backfilled with nitrogen, acetic acid (4 mL) was added and the mixture was stirred at 100 °C for overnight. After cooling down to room temperature, water was added, and the mixture was washed with dichloromethane three times. The organic phase was combined and dried with anhydrous $MgSO_4$. After the removal of the solvent under reduced pressure, the crude product was purified by column chromatography on silica gel with dichloromethane and hexane mixture as eluent yielding **TP-TQ2** as a yellow solid (32 mg, 60.7 %). ^{1}H NMR (400 MHz, $CDCl_3$) δ 8.82 (s, 2H), 8.64 (s, 2H), 8.02 - 7.75 (m, 2H), 7.60 (q, *J* = 5.0 Hz, 2H), 7.41 - 7.27 (m, 6H), 7.20 (d, *J* = 7.7 Hz, 8H), 7.06 - 6.82 (m, 12H), 2.50 (t, *J* = 7.8 Hz, 8H), 1.55 - 1.45 (m, 8H), 1.34 - 1.28 (m, 8H), 0.87 (t, *J* = 6.2 Hz, 12H). ^{13}C NMR (100 MHz, $CDCl_3$) δ 161.37, 151.56, 150.78, 144.46, 143.26, 142.49, 141.40, 139.86, 139.75, 138.52, 135.49, 134.87, 132.47, 130.61, 129.22, 128.45, 128.37, 126.48, 124.90, 124.03, 123.54, 122.86, 122.26, 120.24, 62.99, 35.37, 33.54, 22.70, 14.13.

Preparation of nanoparticles

TP-TQ1, TP-TQ2 and TP-DBBT were each dissolved in tetrahydrofuran along with eight times the mass of F127, and the solutions were rapidly injected into deionized water with high-speed stirring using a microsyringe. The tetrahydrofuran was removed using a rotary evaporator to obtain the corresponding aqueous solutions of nanoparticles.

Fluorescence quantum yield

The absorption and fluorescence spectra of NPs were measured with a Shimadzu UV-Vis-NIR spectroscopy (UV-3600 Plus) and an Edinburgh Instrument spectrofluorometer (FLS1000), respectively. The average particle sizes of NPs were determined by a NICOMP particle sizer instrument (Z3000 plus) equipment at room temperature. The absorption coefficients of molecules and NPs were calculated based on the above calibration curves and Beer-Lambert Law. To measure the QYs of molecules and NPs, the samples and FT-BBT were dispersed in water and toluene at varied concentrations, respectively. The fluorescence intensity of these samples was calculated from the greyscale values of the fluorescence images acquired by Image J. Fluorescence images were obtained by Series III 900/1700-M fluorescence imager under 808 nm excitation (12.5 mW cm^{-2}, 25 ms) with 900LP filter. The integrated area of fluorescent profile was plotted against concentration to obtain the slope. QYs was calculated in the following manner:

$$QYs_{sample} = QYs_{FT-BBT}\frac{Slope_{sample}\ n_{sample}^{2}}{Slope_{FT-BBT}n_{FT-BBT}^{2}}$$

Where QYs_{FT-BBT} in toluene is 19%; the refractive index (n_{water} and $n_{Toluene}$) is 1.3330 and 1.4967, respectively.

Photothermal effect

The photostability of TP-TQ1 NPs in H_2O was explored by monitoring its photothermal effect during five laser on/off cycles with 808 nm laser irradiation (0.5 mW cm^{-2}). TP-TQ1 NPs aqueous solution (100 μg mL^{-1}) was exposed to an 808 nm laser at 0.5 W cm^{-2} for 10 min (laser on), and then cooled naturally for 10min (laser off). This laser on/off cycle was repeated five times. TP-TQ2 NPs and TP-DBBT NPs aqueous solution were irradiated at 808 nm laser irradiation (0.5 W cm^{-2}) for 10 min. A portable infrared thermometer was employed to record the temperature at 20 s intervals in these procedures. The photothermal conversion efficiency was calculated by the following equation:

$$PCE = \frac{\frac{m_D C_D}{\tau_s}\Delta T_{max} - Q_S}{I(1 - 10^{-A})}$$

Where ΔT_{max} is the temperature change of NPs aqueous solution at the maximum steady-state temperature, τ_s is the sample-system time constant, m_D and C_D are the mass and heat capacity (4.2 J g^{-1}) of the H_2O used as the solvent, Q_S is the heat associated with light absorption by the solvent. The I is the laser power, A is absorbance of the NPs aqueous solution at 808 nm.

MTT assay

The metabolic viability of 4T1 cells was evaluated by Cell Viability Kit 3-(4,5- dimethylthiazol-2-yl)-2,5-diphenyltetrazolium bromide (MTT) assay. 4T1 cells were incubated in DMEM medium containing 10% FBS and 1% antibiotics (penicillin− streptomycin, 10000 U/mL). All cells were cultured at 37°C in a humidified atmosphere containing 5% CO_2 and 95% air. The cells were seeded in two 96-well plates at a density of 5×10^3 cells/well labelled with No Laser and Laser. After culture in the incubator for 24 h, the old medium was replaced using 100 μL of TP-TQ1 NPs solutions at

concentrations of 0, 10, 20, 30, 40, 50, 60, 70, 80, 90 μg mL^{-1}. Upon incubation for another 24 h, 20 μL of MTT solution was added and incubated in 37 °C for 4 hours to evaluate the dark cytotoxicity of TP-TQ1 NPs. Furthermore, cells were also exposed to 808 nm laser irradiation (0.5 W cm^{-2}) for 5 min and incubated for 20 h for photothermal cytotoxicity study under the same experimental conditions. Then 150 μL DMSO were added into each well, the absorbance at 490 nm from each well was recorded by a microplate reader (Varioskan LUX). The cell viability was expressed by the ratio of absorbance from the cells treated with NPs to that of the cells incubated with culture medium only.

Live-dead co-staining

4T1 cells were added to 24-well plates (5×10^3 cells/well). After incubation for 24 h, cells were incubated with TP-TQ1 NPs at a concentration of 0 and 100 μg mL^{-1} with or without the laser at each concentration under two conditions and the cells were continuously incubated for 6 h. Then, the cells were rinsed twice with PBS. Afterwards, the 4T1 cells were stained using a calcein AM/PI Detection Kit. The live and dead cells were then imaged under a fluorescence microscope (NIB900).

Tumor model

The female Balb/c mice (14-18 g weight, five weeks aged) were purchased from Comparative Medicine Centre of Yangzhou University. All animal experiments were approved and guided by the Zhejiang Provincial People's Hospital, Affiliated People's Hospital, Hangzhou Medical College, in compliance with the relevant laws and institutional guidelines. The 4T1 cells were inoculated on the left rear leg of the mice with 50 μL of PBS containing 4×10^6 cells. When the tumor volumes approached 100-150 mm^3, the mice were used to carry out the following *in vivo* experiments.

NIR-II fluorescence imaging

Nude mice were anaesthetised using a gas anaesthesia system after injection of TP-TQ1 NPs (2 mg mL^{-1}, 150 μL) via a tail vein. The fluorescence signal from blood vessels was detected and recorded under a NIR-II imaging instrument equipped with an 808 nm laser (1100 nm long-pass filter, 50 mW cm^{-2}, and 200 ms exposure time).

4T1 tumor-bearing BALB/c mice were removed the hair on the back before imaging tests were performed. After injection of TP-TQ1 NPs (2 mg mL^{-1}, 150 μL) via a tail vein, Balb/c mice were anaesthetized using a gas anesthesia system. The fluorescence signal from the tumor site at various time was detected and recorded under a NIR-II imaging instrument equipped with an 808 nm laser (1000 nm long-pass filter, 25 mW cm^{-2}, and 200 ms exposure time). The fluorescence intensity of these images was calculated from the greyscale values of the fluorescence images acquired by Image J.

Photothermal imaging

4T1 tumor-bearing BALB/c mice were removed the hair on the back before imaging tests were performed. After 24 h post-injection of TP-TQ1 NPs (2 mg mL^{-1}, 150 μL)/PBS via a tail vein, the temperature of tumor site was monitored and recorded at various time using a thermal imaging camera under 808 laser irradiation (0.5 W cm^{-2}, 5 min).

Photoacoustic imaging

Nude mice were anaesthetized using a gas anesthesia system after injection of TP-TQ1 NPs (2 mg mL^{-1}, 150 μL) via a tail vein. The photoacoustic signal intensity of the tumor in nude mice was

calculated from the greyscale values of the photoacoustic images acquired by Image J. The photoacoustic images at various time were obtained by TomoWave LOIS-3D photoacoustic imager under 808 nm laser excitation. The maximum laser output energy 400 mJ, pluse duration 3~6 ns.

In vivo photothermal therapy

The 4T1 tumor bearing mice were randomly divided into three groups (PBS + Laser, NPs, and NPs + Laser, n = 5/group). The mice of PBS + Laser group were injected with PBS (150 μL), the mice of NPs and NPs + Laser were injected with TP-TQ1 aqueous solution (2.0 mg/mL, 150 μL). After 24 h of drug administration, the solid tumors of PBS and NPs + Laser groups were irradiated for 5 min with an 808 nm laser (0.5 W cm^{-2}). The body weight and tumor volumes of each group were recorded in every two days by a digital scale and caliper, respectively. The tumor volume was calculated by formula of length × width× width/2. To check the *in vivo* biocompatibility of the TP-TQ1 NPs, after 15 days, the mouse of each group was randomly chosen and euthanized to collect organs (including the heart, liver, spleen, lung, and kidney) for H&E staining.

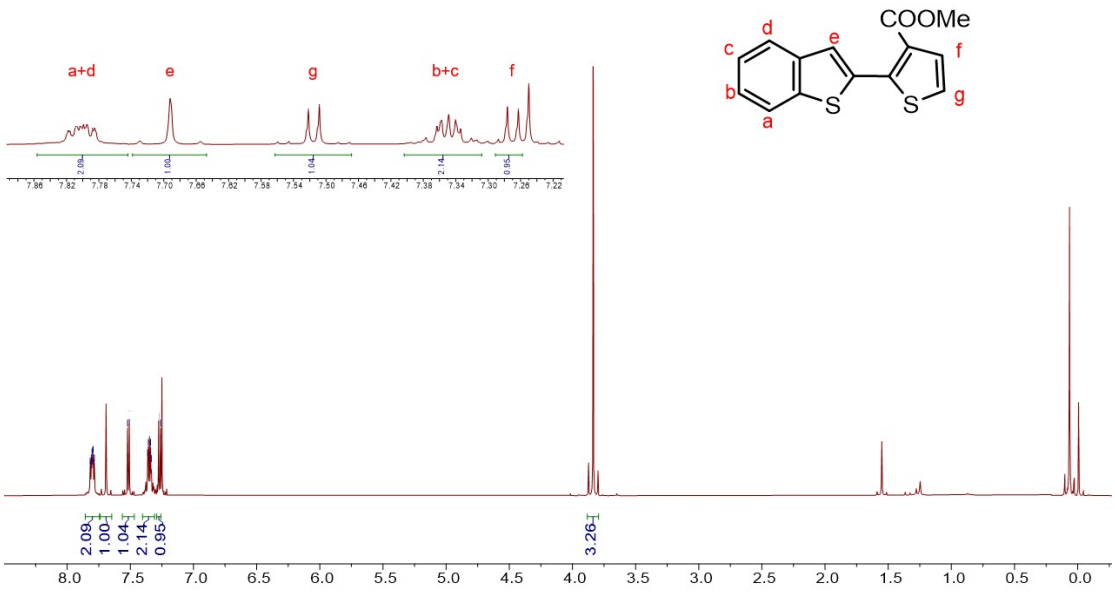

Figure S1. ^{1}H NMR spectrum of compound 1.

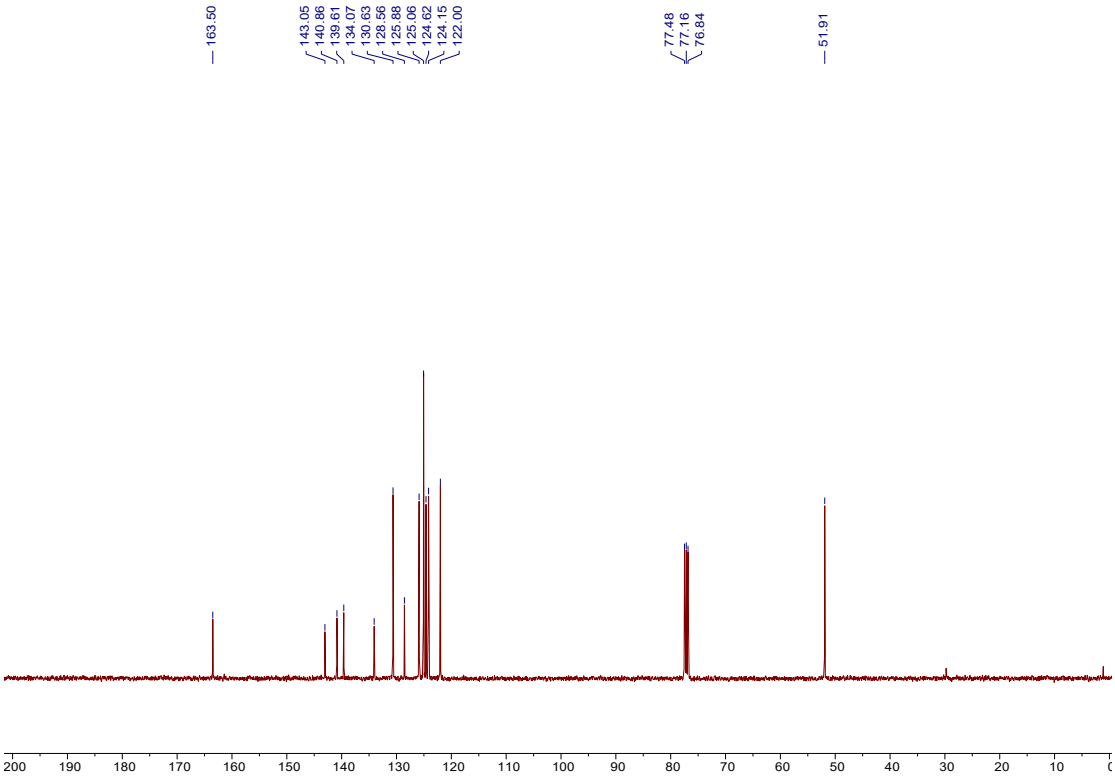

Figure S2. ^{13}C NMR spectrum of compound 1.

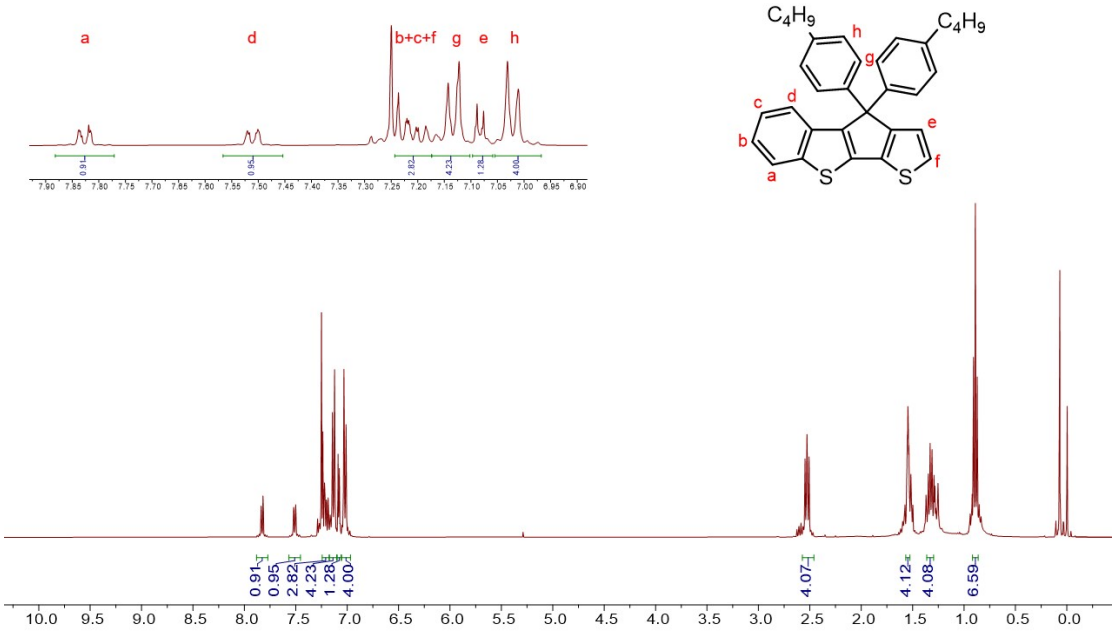

Figure S3. ^{1}H NMR spectrum of compound 2.

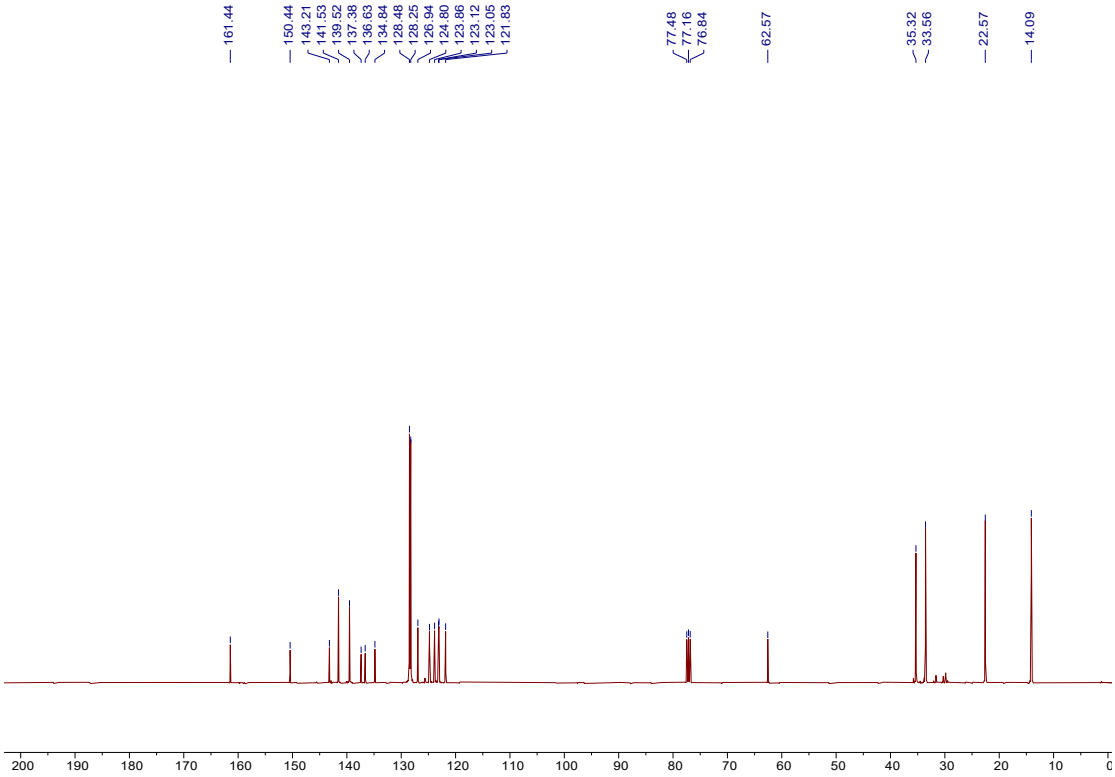

Figure S4. ^{13}C NMR spectrum of compound 2.

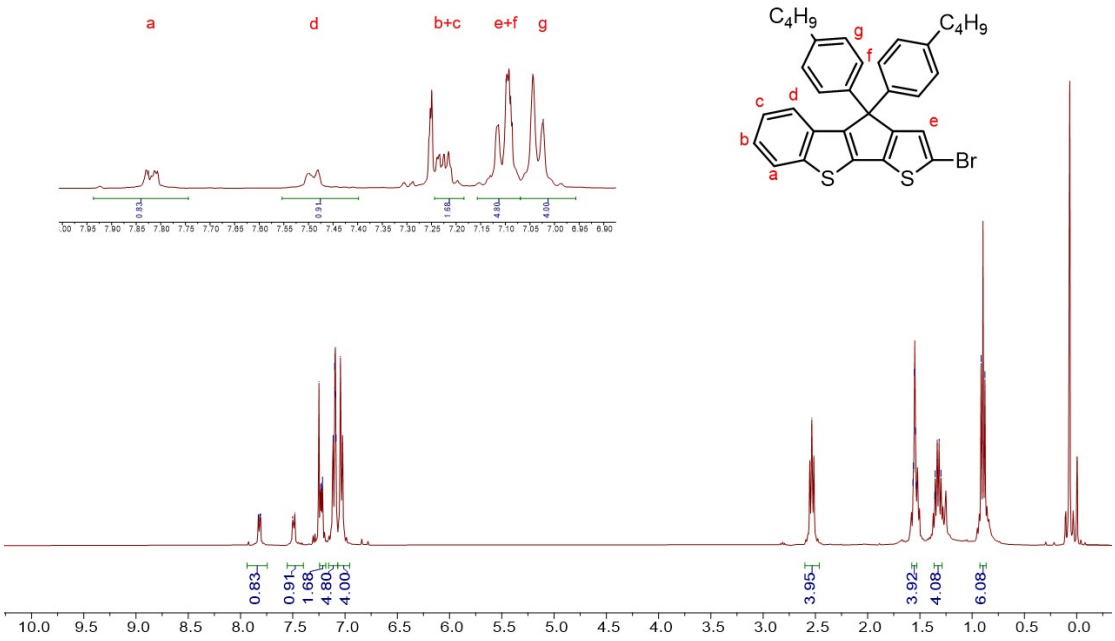

Figure S5. ^{1}H NMR spectrum of compound 3.

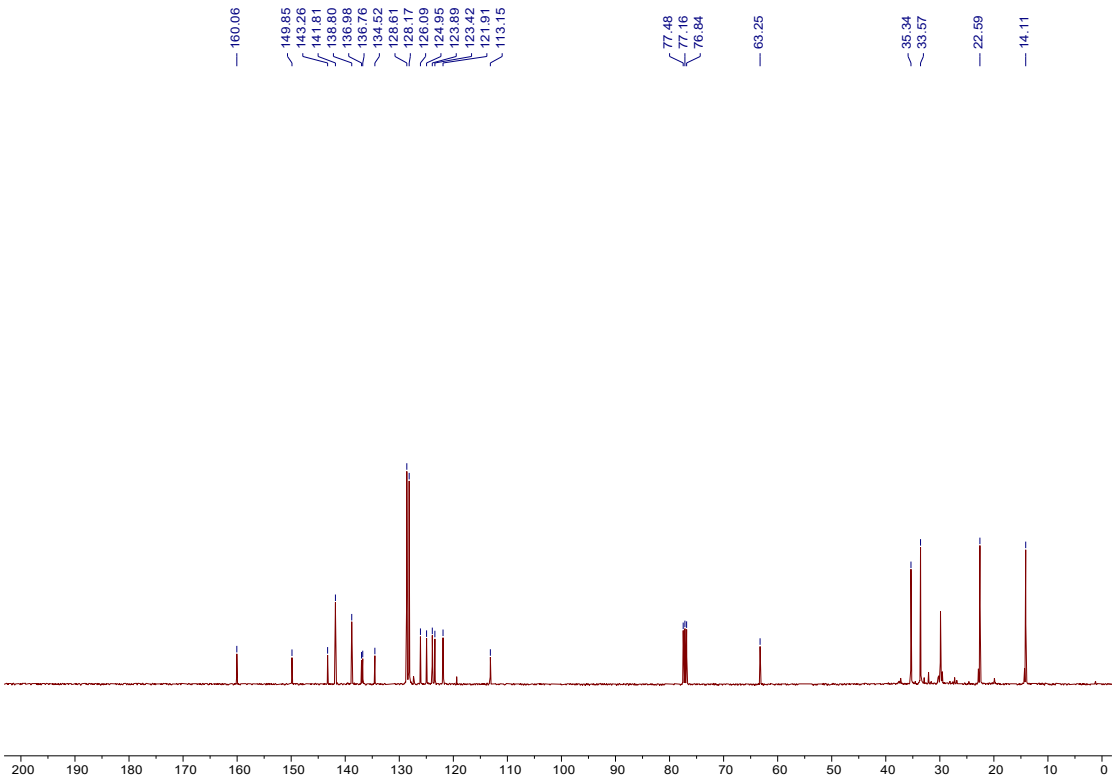

Figure S6. ^{13}C NMR spectrum of compound 3.

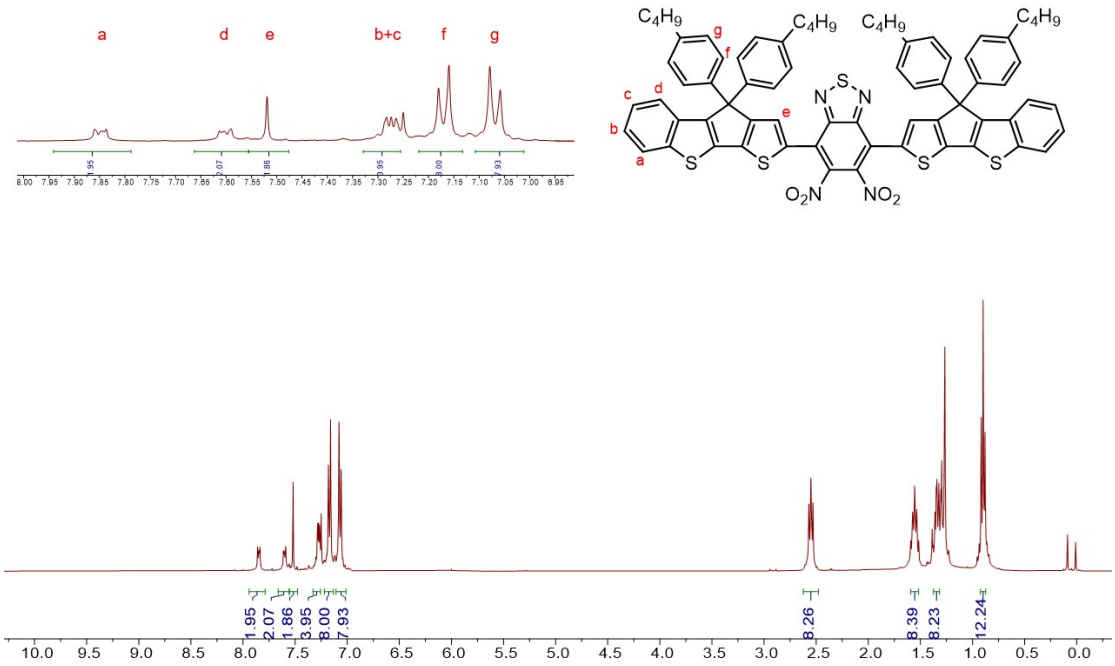

Figure S7. ^{1}H NMR spectrum of compound 6.

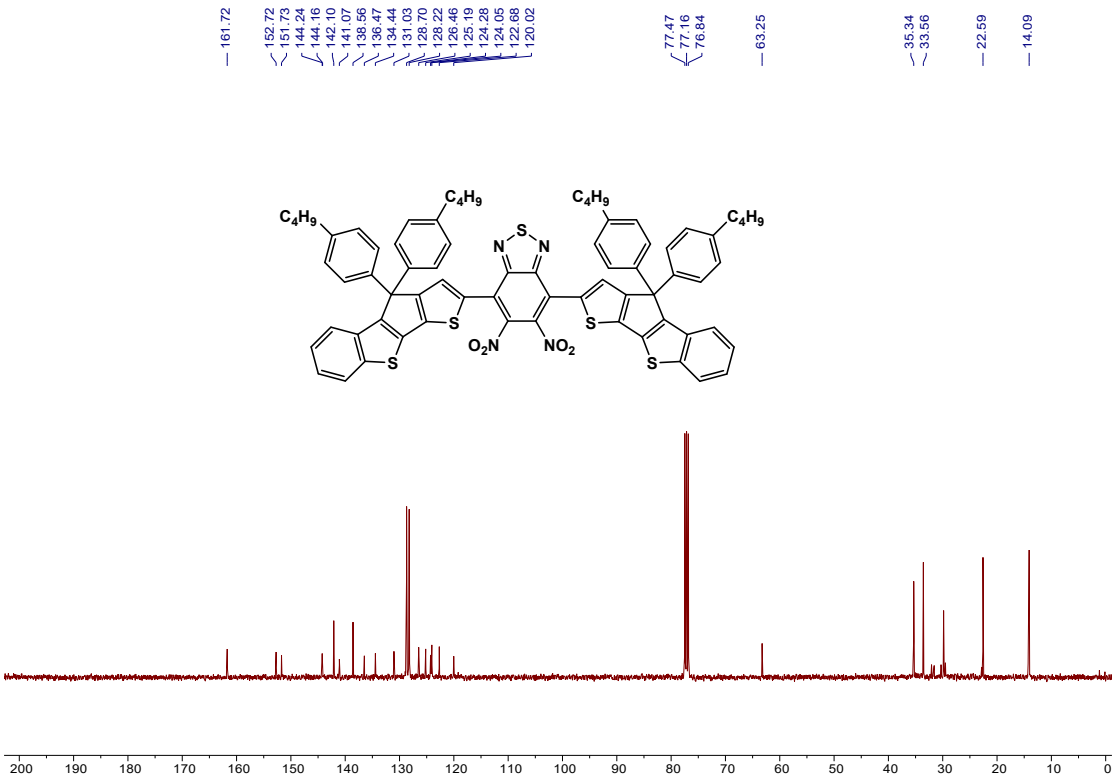

Figure S8. ^{13}C NMR spectrum of compound 6.

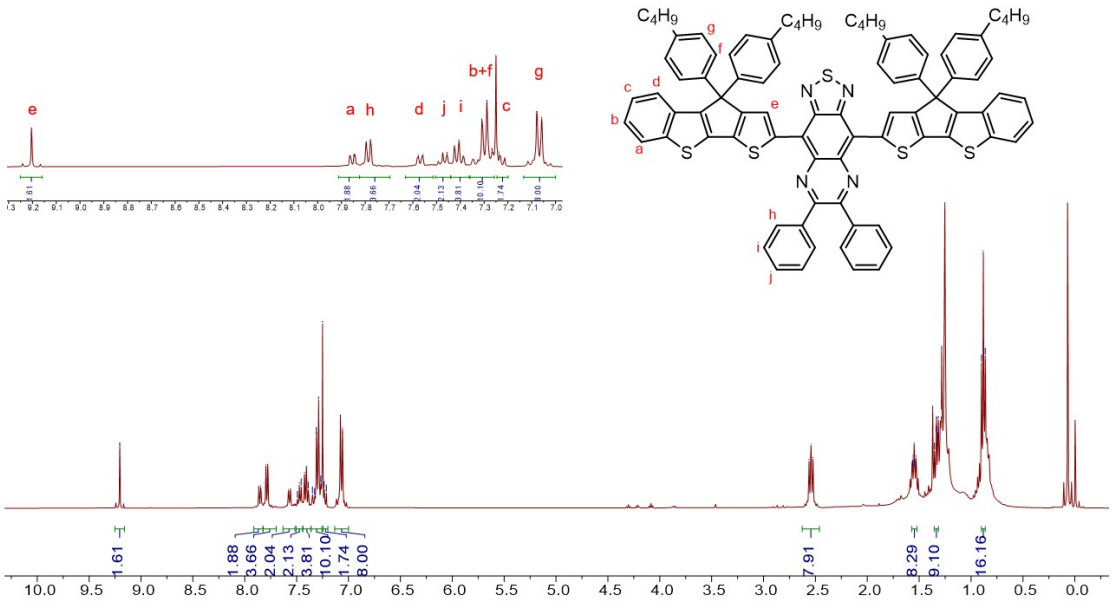

Figure S9. ^{1}H NMR spectrum of compound TP-TQ1.

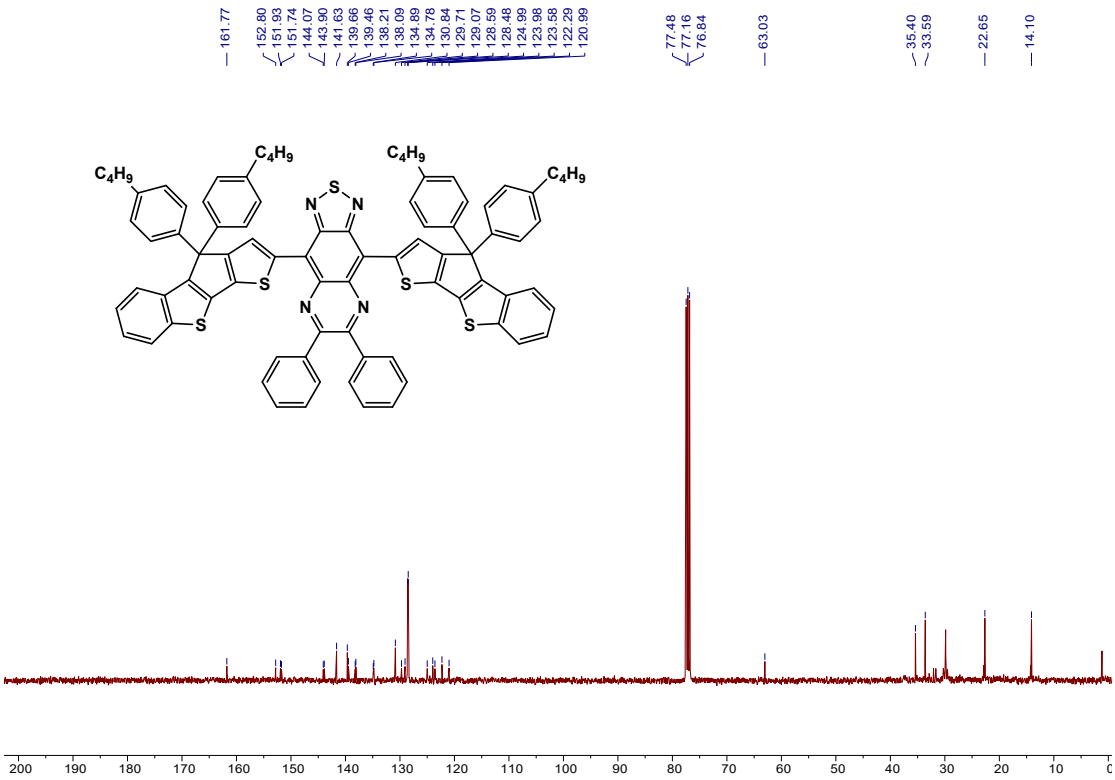

Figure S10. ^{13}C NMR spectrum of compound TP-TQ1.

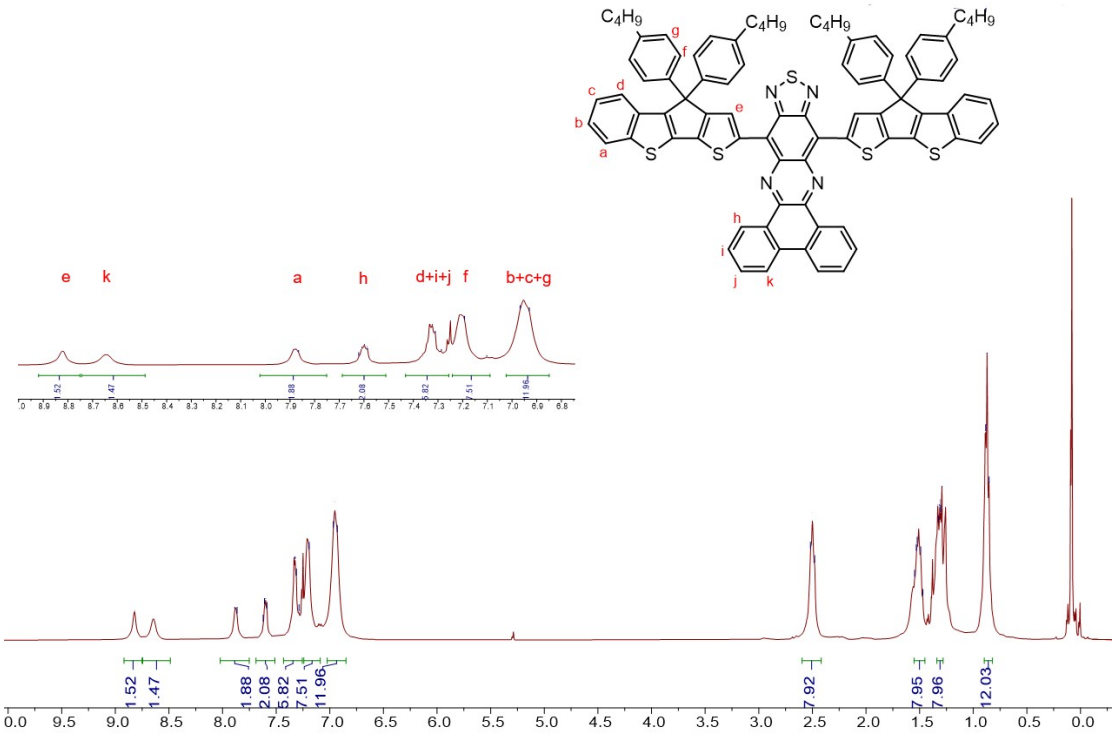

Figure S11. ^{1}H NMR spectrum of compound TP-TQ2.

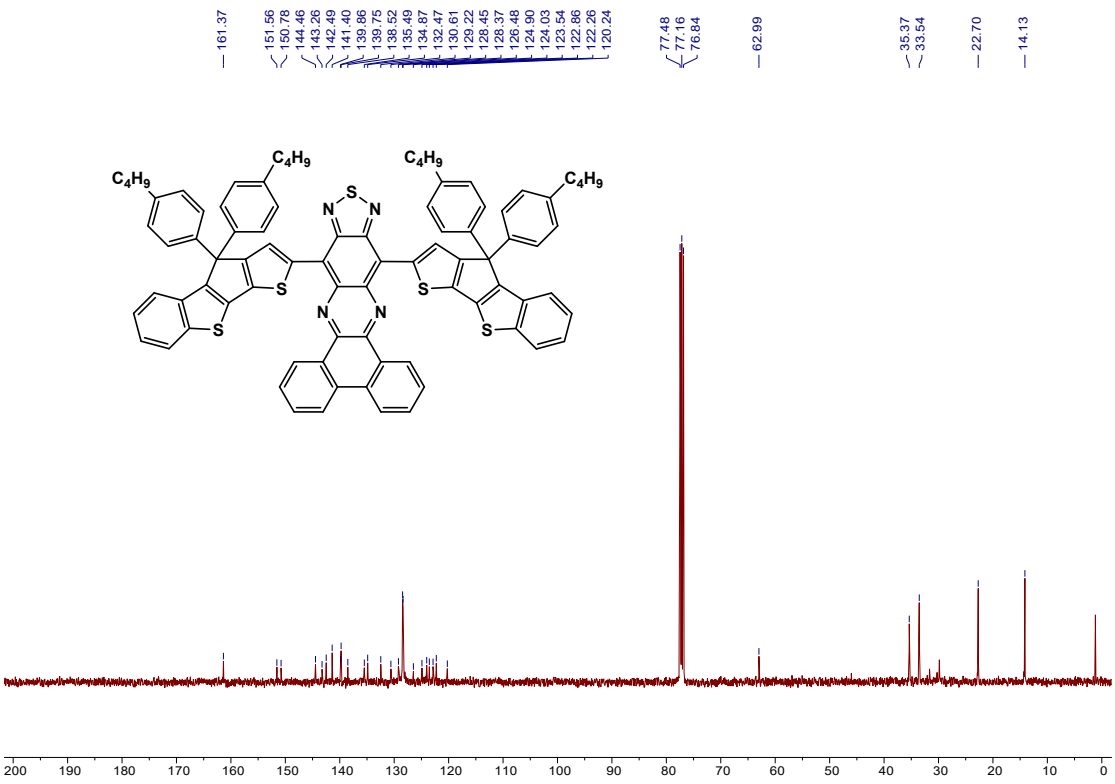

Figure S12. ^{13}C NMR spectrum of compound TP-TQ2.

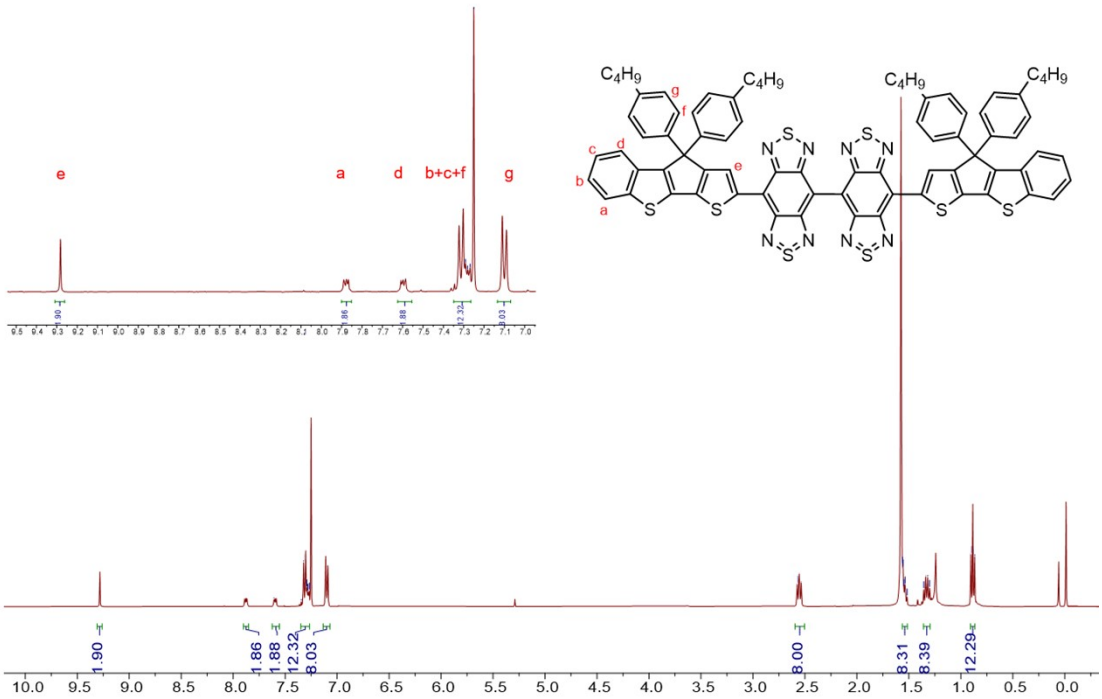

Figure S13. ^{1}H NMR spectrum of compound TP-DBBT.

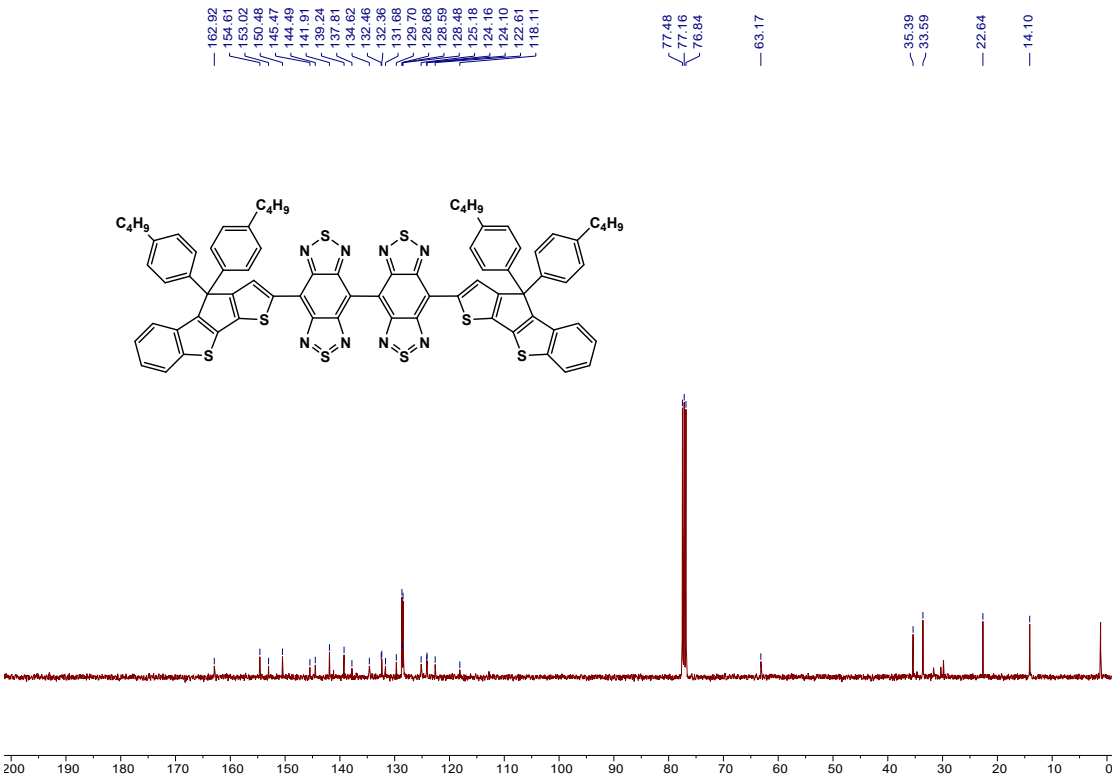

Figure S14. ^{13}C NMR spectrum of compound TP-DBBT.

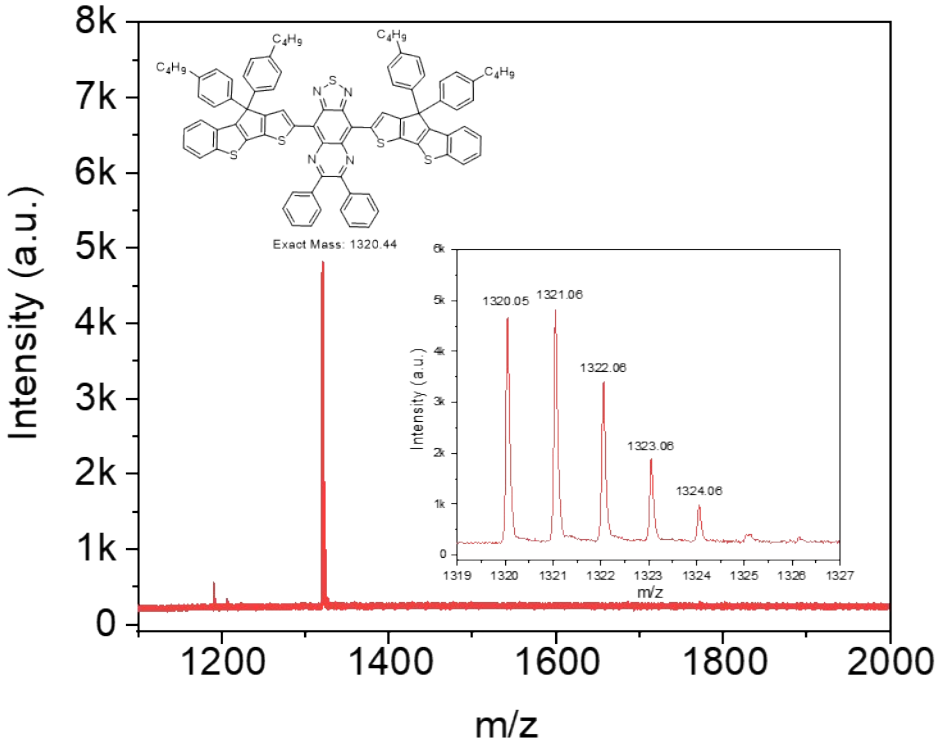

Figure S15. MALDI-TOF-MS spectrum of compound TP-TQ1.

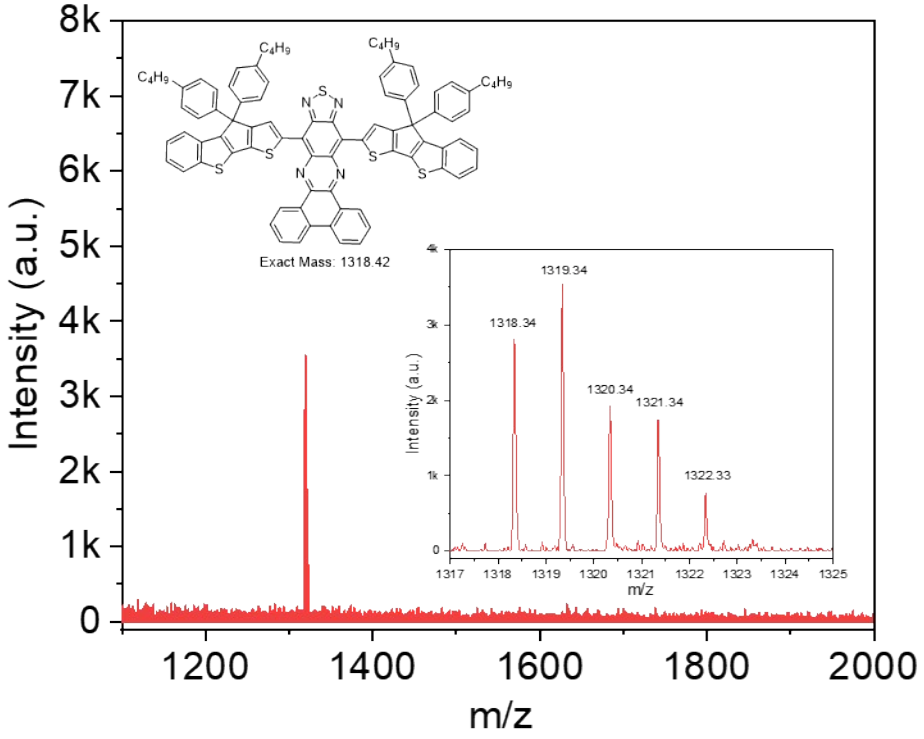

Figure S16. MALDI-TOF-MS spectrum of compound TP-TQ2.

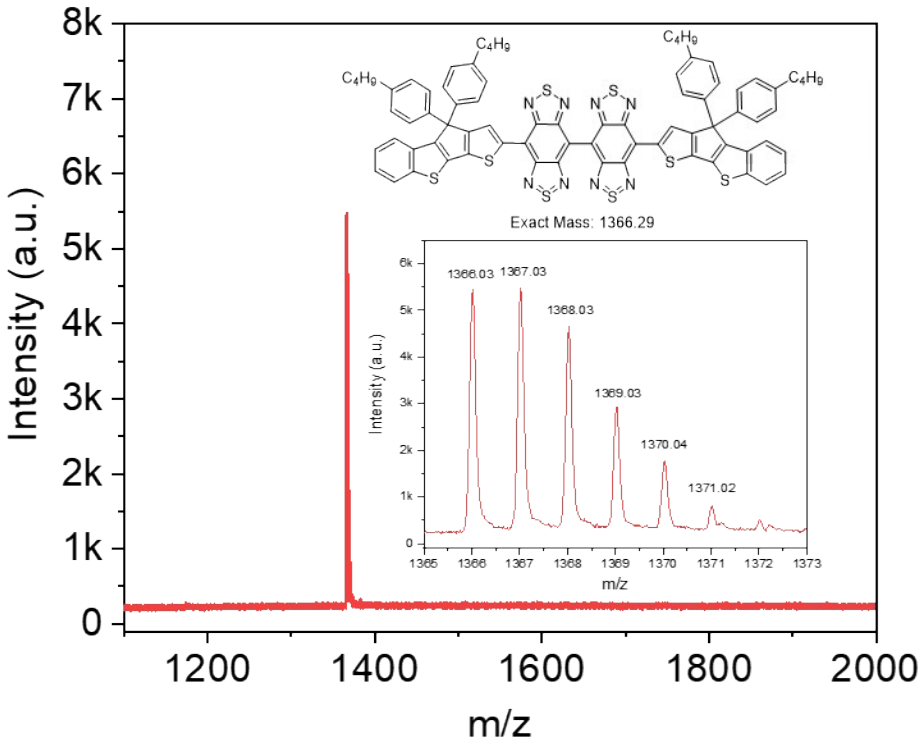

Figure S17. MALDI-TOF-MS spectrum of compound TP-DBBT.

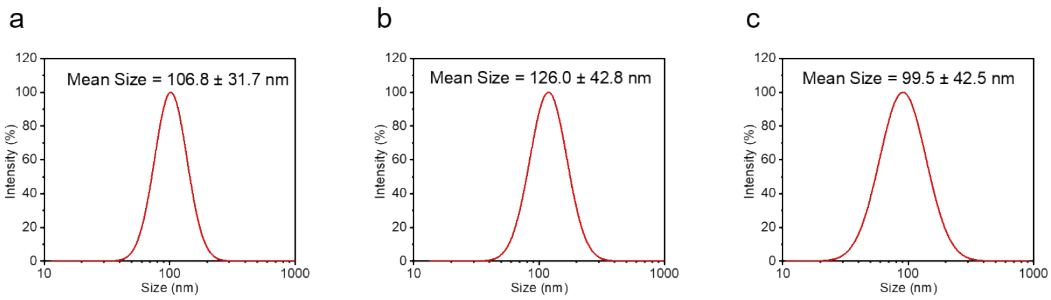

Figure S18. Dynamic light scattering results of (a) TP-TQ1 NPs, (b) TP-TQ2 NPs and (c) TP-DBBT NPs.

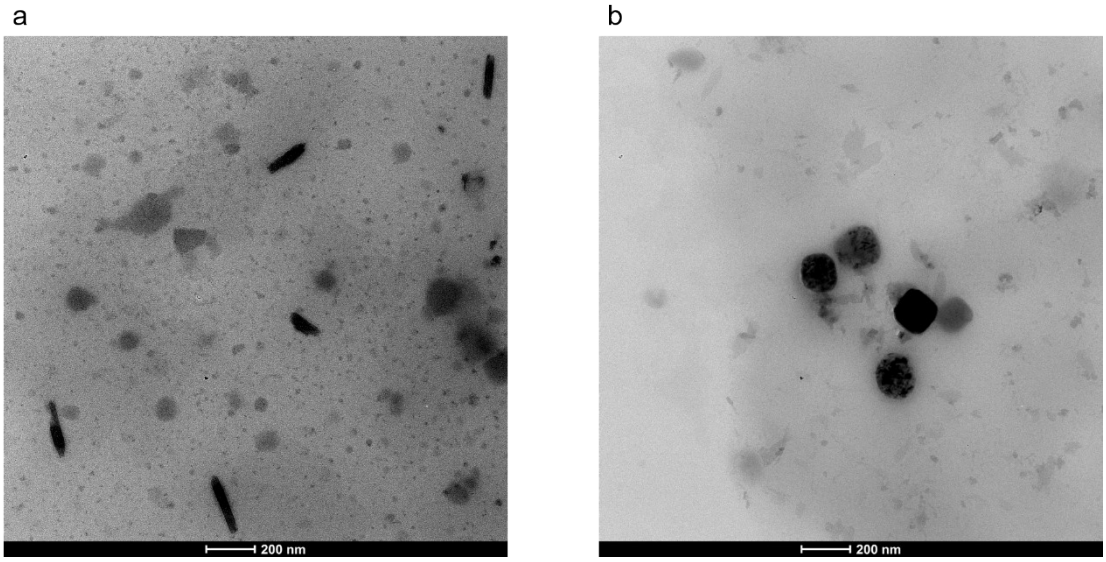

Figure S19. Transmission electron microscopy (TEM) image of TP-TQ1 NPs (a) and TP-TQ2 NPs (b).

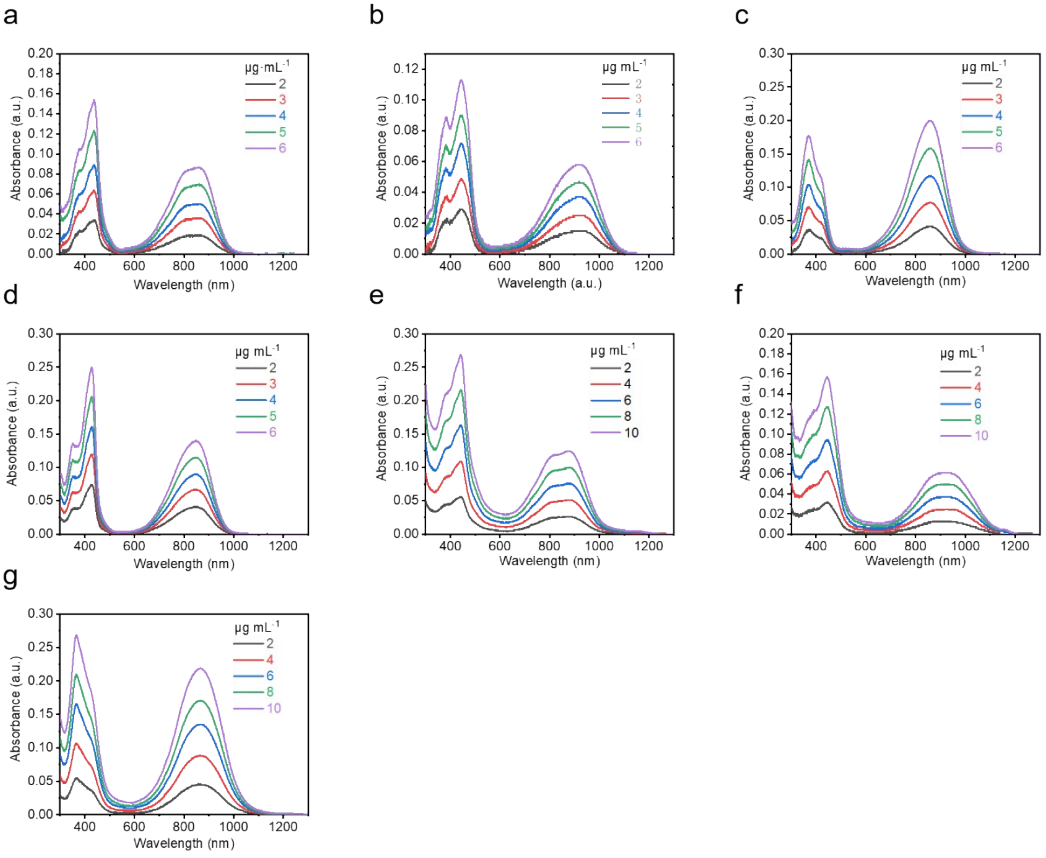

Figure S20. Absorption spectra of TP-TQ1 (a), TP-TQ2 (b), TP-DBBT (c) and FT-BBT (d) in toluene with different concentrations (2, 3, 4, 5, 6 μg mL^{-1}), respectively; Absorption spectra of TP-TQ1 NPs (e), TP-TQ2 NPs (f) and TP-DBBT NPs (g) in H_2O with different concentrations (2, 4, 6, 8, 10 μg mL-

[1]), respectively.

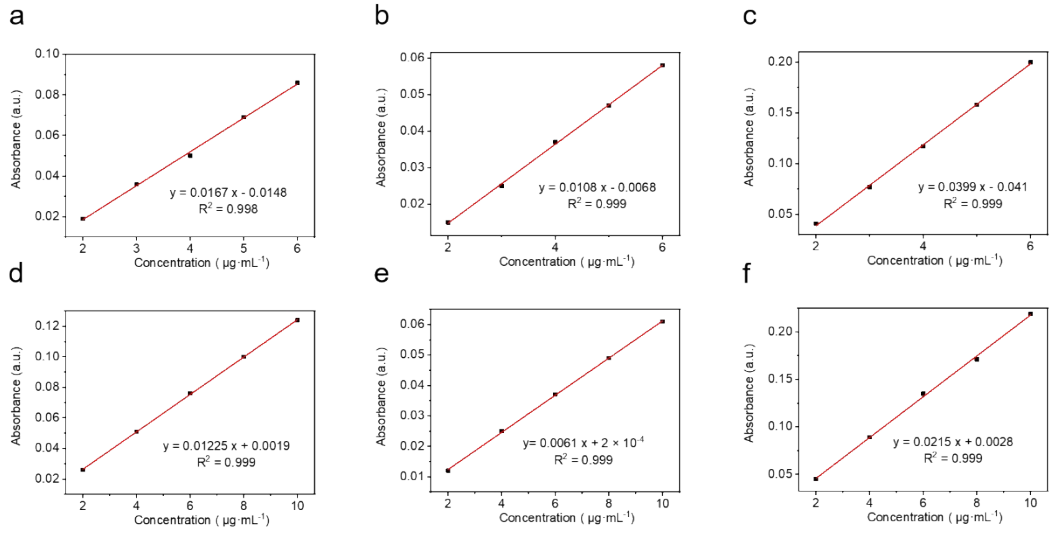

Figure S21. Linear-fitted slopes of absorption values at the maximum absorption peaks of TP-TQ1 (a), TP-TQ2 (b) and TP-DBBT (c) in toluene versus the corresponding concentration values; Linear-fitted slopes of the integrated fluorescence intensities of TP-TQ1 NPs (d), TP-TQ2 NPs (e) and TP-DBBT NPs (f) in H_2O versus the corresponding concentration values.

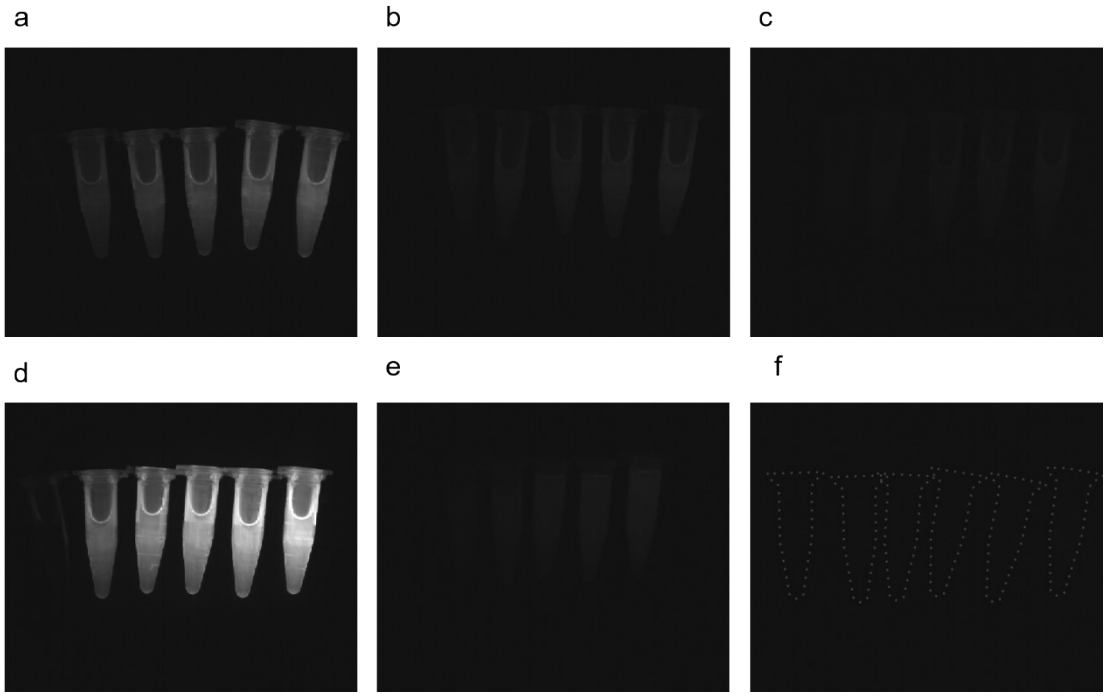

Figure S22. Fluorescence images of TP-TQ1 (a), TP-TQ2 (b), TP-DBBT (c) and FT-BBT (d) in toluene

with different concentrations (2, 3, 4, 5, 6 μg mL^{-1}) under 808 nm excitation (900 LP filter, 12.5 mW cm^{-1}, exposure time 25 ms), respectively; Fluorescence images of TP-TQ1 NPs (e) and TP-TQ2 NPs (f) in H_2O with different concentrations (2, 4, 6, 8, 10 μg mL^{-1}) under 808 nm excitation (900 LP filter, 12.5 mW cm^{-1}, exposure time 25 ms), respectively.

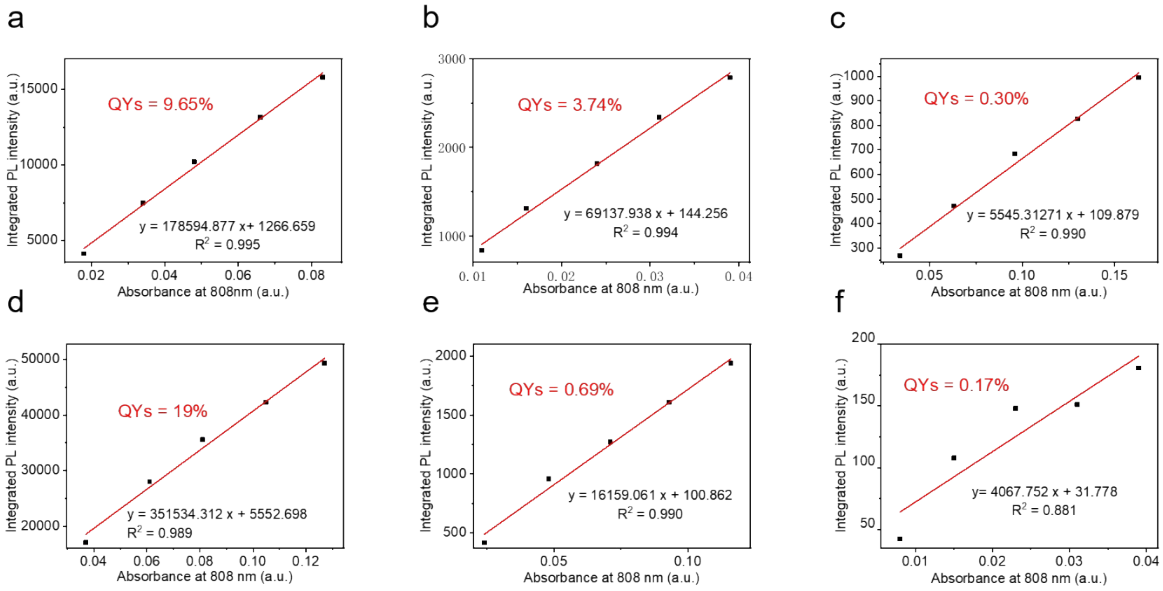

Figure S23. Determination of QYs. Linear-fitted slopes of the integrated fluorescence intensities of TP-TQ1 (a), TP-TQ2 (b), TP-DBBT (c) and FT-BBT (d) in toluene above 900 nm versus the corresponding absorption values at 808 nm; Linear-fitted slopes of the integrated fluorescence intensities of TP-TQ1 NPs (e) and TP-TQ2 NPs (f) in H_2O above 900 nm versus the corresponding absorption values at 808 nm.

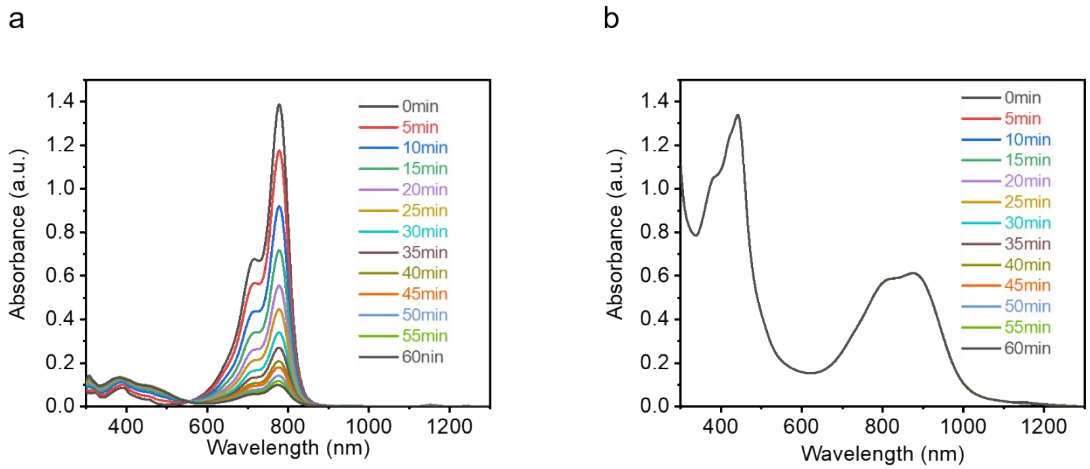

Figure S24. Absorption spectra of TP-TQ1 NPs (60 μg mL^{-1}) and ICG (6 μg mL^{-1}) in water after continuous irradiation at different time points with 808 nm laser (0.4 W cm^{-2}). The absorbance of ICG gradually decreases over time, indicating instability of ICG under laser irradiation.

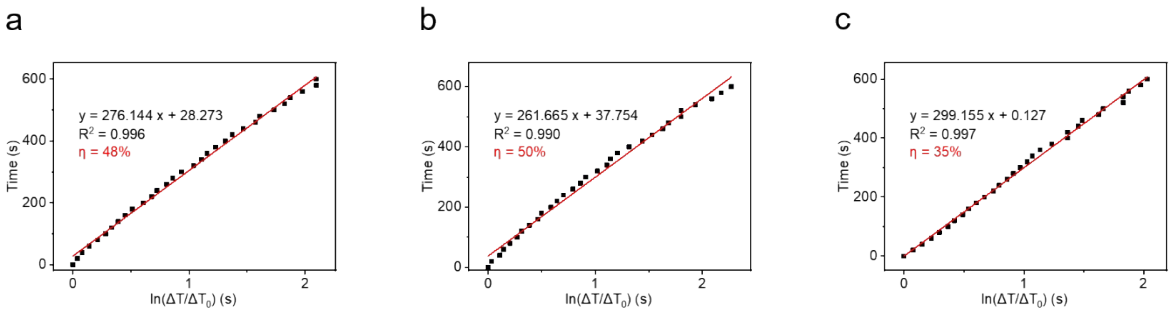

Figure S25. Determination of PCE. The time constant for TP-TQ1 NPs (a), TP-TQ2 NPs (b)and TP-DBBT NPs (c) heat transfer from the system.

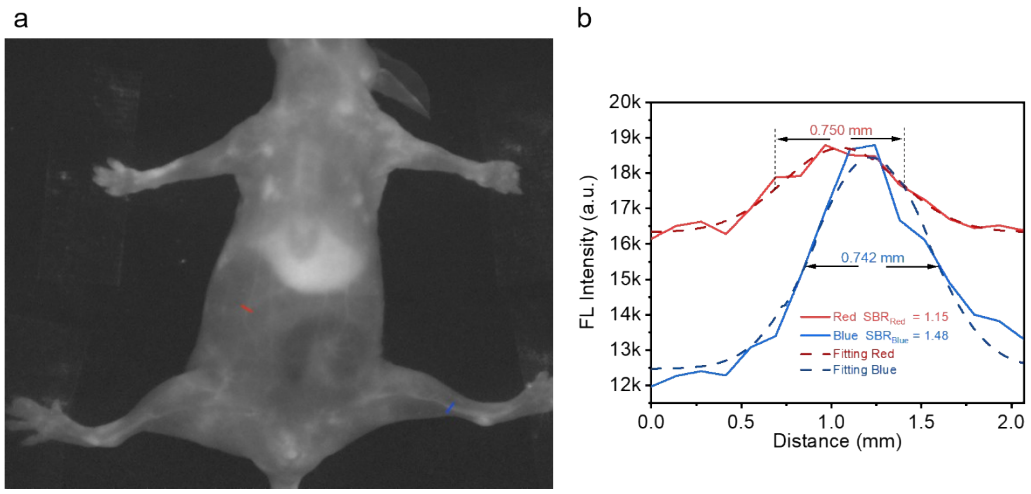

Figure S26. (a) In vivo NIR-II blood vessels images of nude mice intravenous injection with TP-TQ1 NPs using an 1100 nm long-pass filter (808 nm laser, 50 mW cm^{-2}, and 200 ms exposure time). (b) The corresponding cross-sectional fluorescence intensity profiles along red/blue lines in (a). The dashed curves in the diagrams below represent a Gaussian fit to the data.

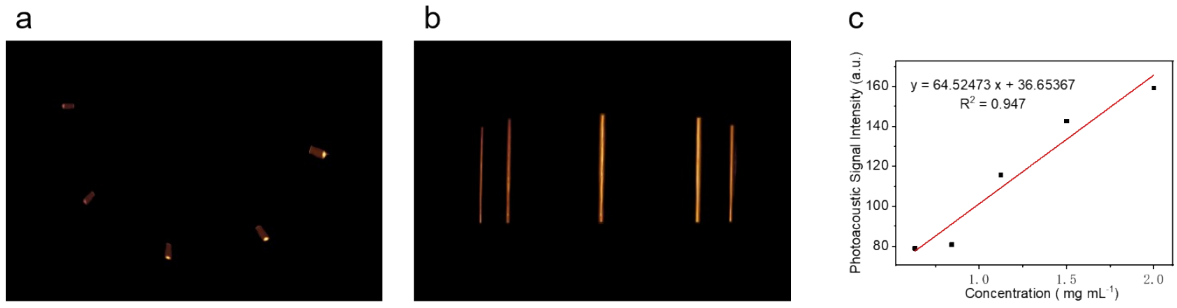

Figure S27. (a, b) Photoacoustic imaging of TP-TQ1 NPs at varied concentrations showed a positive correlation between photoacoustic signal intensity and concentration. (c) Fitting curve plot of TP-TQ1 NPs at varied concentrations under 808 nm laser irradiation.

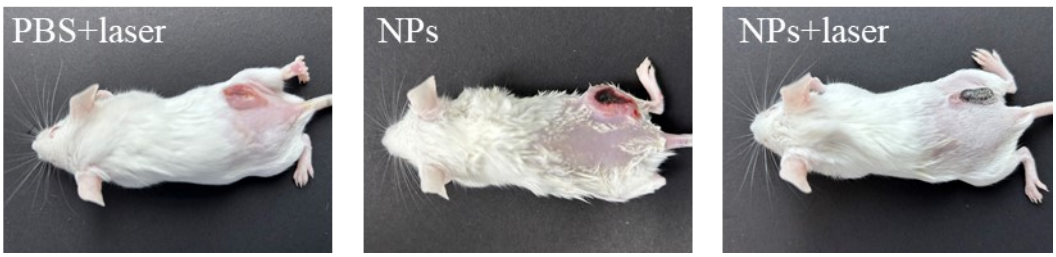

Figure S28. Photo images of mice of different treatment groups after 14 days treatment.

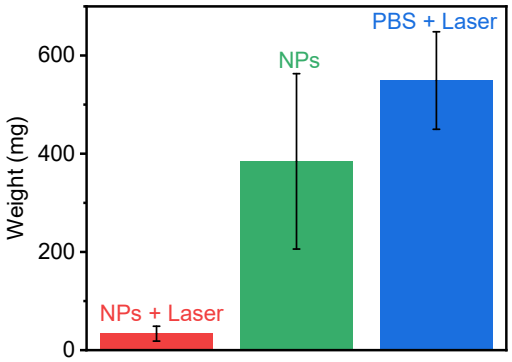

Figure S29. Tumor weights from sacrificed mice on the 15th day

Table S1. Optical properties of the TQ-based molecules and NPs

	$\lambda_{abs,max}$ [a]	$\lambda_{em,max}$ [b]	Stokes shift	ε [c]	QY [d]	Ref.
	(nm)	(nm)	(nm)	(L mol^{-1} cm^{-1})	(%)	
TQ-BPN dots	630	810	180	/	2.8	1
DPTQ-PTZ NPs	639	928	289	/	0.059	2
DPTQ-PhPTZ	646	926	280	8700	0.092	3
TTQ-DP NPs	648	896	248	16000	9.88	4
DPTQ-PhPXZ	655	911	256	9700	0.14	3
MGNPs	681	915	234	/	1.3	5
TTQP NPs	711	1050	339	32900	0.47	4
TTQT NPs	730	1152	422	25700	2.6	6
TTQ-F@NPs	733	1060	327	/	/	7
TTQ-SF@NPs	735	1037	302	7941	0.84	8
TBP-b-DFA NPs	740	909	169	4100	/	9
TTQPL NPs	745	1092	347	31200	1.5	6
TTQiT NPs	755	1102	347	36600	3.7	6
FT-TQT (H2O)	770	1034	264	/	0.49	10
TTQ-F-PEG (H2O)	792	1073	281	/	/	7
TTQ-TC (THF)	796	1042	246	21115	18.3	11
DPBTA-DPTQ NPs	817	1125	308	/	0.45	12
DHTDP NP	840	1050	210	/	/	13
DTP-DPTQ NPs	852	1120	268	/	0.01	14
O-T NPs	857	/	/	15500	0.038	15
O-BT NPs	845	1056	211	36500	0.35	16

TP-TQ1	877	1032	155	16175	0.69	**This work**

[a] $\lambda_{abs,max}$ is peak of maximum absorption; [b] $\lambda_{em,max}$ is peak of maximum emission; [c] ε is molar extinction coefficient; [d] quantum yield.

References

1. J. Qi, C. Sun, A. Zebibula, H. Zhang, R. T. K. Kwok, X. Zhao, W. Xi, J. W. Y. Lam, J. Qian and B. Z. Tang, *Adv. Mater*., 2018, **30**, 1706856.

2. Li, C. Yin, R. Wang, Q. Fan, W. Wu and X. Jiang, *ACS Appl. Mater. Interfaces*, 2020, **12**, 20281-20286.

3. S. Li, T. Cheng, C. Yin, S. Zhou, Q. Fan, W. Wu and X. Jiang, *ACS Appl. Mater. Interfaces*, 2020, **12**, 43466-43473.

4. Y. Li, M. Zha, G. Yang, S. Wang, J.-S. Ni and K. Li, *Chem. – Eur. J.*, 2021, **27**, 13085-13091.

5. Y. Qin, X. Li, S. Lu, M. Kang, Z. Zhang, Y. Gui, X. Li, D. Wang and B. Z. Tang, *ACS Mater. Lett.*, 2023, **5**, 1982-1991.

6. Y. Li, M. Zha, T. Kang, C. Li, X. Wu, S. Wang, S.-B. Lu, Y.-S. Lee, Y.-R. Wu, J.-S. Ni and K. Li, *Small*, 2022, **18**, 2105362.

7. K. He, S. Chen, Y. Chen, J. Li, P. Sun, X. Lu, Q. Fan and W. Huang, *ACS Appl. Polym. Mater.*, 2021, **3**, 3238-3246.

8. K. He, S. Chen, W. Xu, X. Tai, Y. Chen, P. Sun, Q. Fan and W. Huang, *Biomater. Sci.*, 2021, **9**, 6434-6443.

9. Y. Li, X. Fan, Y. Li, S. Liu, C. Chuah, Y. Tang, R. T. K. Kwok, J. W. Y. Lam, X. Lu, J. Qian and B. Z.

Tang, *ACS Nano*, 2022, **16**, 3323-3331.

10. A. Ji, H. Lou, C. Qu, W. Lu, Y. Hao, J. Li, Y. Wu, T. Chang, H. Chen and Z. Cheng, *Nat. Commun*., 2022, **13**, 3815.

11. S. Chen, B. Sun, H. Miao, G. Wang, P. Sun, J. Li, W. Wang, Q. Fan and W. Huang, *ACS Mater. Lett.*, 2020, **2**, 174-183.

12. D. Yan, W. Xie, J. Zhang, L. Wang, D. Wang and B. Z. Tang, *Angew. Chem. Int. Ed.*, 2021, **133**, 26973-26980.

13. J. Cui, F. Zhang, D. Yan, T. Han, L. Wang, D. Wang and B. Z. Tang, *Adv. Mater.*, 2023, **35**, 2302639.

14. P. Xiao, Y. Sun, M. Liang, S. Yang, J. Li, L. e. Zhang, X. Jiang and W. Wu, *Mater. Today Nano*, 2023, **24**, 100404.

15. J. Liu, Y. Xiong, Y. Gao, X. Xu, K. Chen, Q. Shen, W. Huang, Q. Fan and Q. Wang, *Small*, 2023, **19**, 2205640.

16. Q. Wang, J. Liu, X. Zhang, Y. Tang, Y. Xiong, L. Zhang, T. Xiao and Q. Fan, *Chem. Commun.*, 2023, **59**, 9611-9614.